Kinetic and structural studies on 'tethered' Ru(II) arene ketone reduction catalysts

Fung Kei (Kathy) Cheung,[a] Adam J. Clarke,[a] Guy J. Clarkson,[a] David J. Fox,[a] Mark A. Graham,[b] Changxue Lin,[a] Adriana Lorente Crivillé[a] and Martin Wills[a]*

Received (in XXX, XXX) Xth XXXXXXXXX 200X, Accepted Xth XXXXXXXXX 200X
First published on the web Xth XXXXXXXXX 200X
DOI: 10.1039/b000000x

A series of kinetic and structural investigations on ruthenium-based catalysts for asymmetric transfer hydrogenation (ATH) of ketones are reported. A method is reported for monitoring the formation of ruthenium hydride species in real time using ^{1}H NMR spectroscopy.

Asymmetric transfer hydrogenation (ATH) of ketones using formic acid/triethylamine (FA/TEA), provides an efficient method for the enantioselective synthesis of alcohols.[1-6] A number of Ru(II) complexes of monotosylated diamines have given excellent results for a range of substrates, including imines[4] and ketones.[2,3,5,6] In recent work, we have demonstrated that stereochemically well-defined complexes containing a 'tether' between the arene and chiral diamine give excellent results in terms of activity and enantioselectivity for the reduction of acetophenone derivatives and heterocyclic ketones (Scheme 1).[5] A series of derivatives **1-6**, based on the untethed parent compound **7** described by Noyori *et al.*[2] were prepared and the kinetics of acetophenone reduction were measured. In this paper we report the results of further investigations into the mechanism by which these 'tethered' catalysts operate.

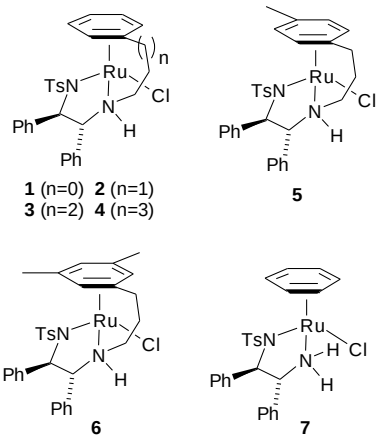

Figure 1: Structures of 'tethered' ATH catalysts investigated in this study.

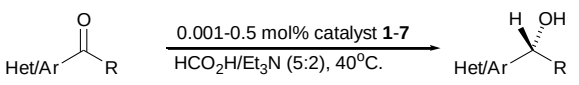

Scheme 1: Asymmetric ketone reduction using Ru(II) catalysts **1-7**.

A kinetic model was developed for the reduction mechanism (Scheme 2), consisting of three forms of the catalyst in a three-step catalytic cycle. The Ru-hydride **8** ('Ru-H') is formed from the chloride pre-catalyst. Hydride **8** reduces acetophenone with a rate constant of k_1 to give 16 electron species **9** ('Ru'). Rapid abstraction of hydrogen from formic acid by **9** generates formate complex **10** ('Ru-FA'), from which CO_2 is eliminated with a rate constant of k_2 to regenerate Ru-hydride **8**.

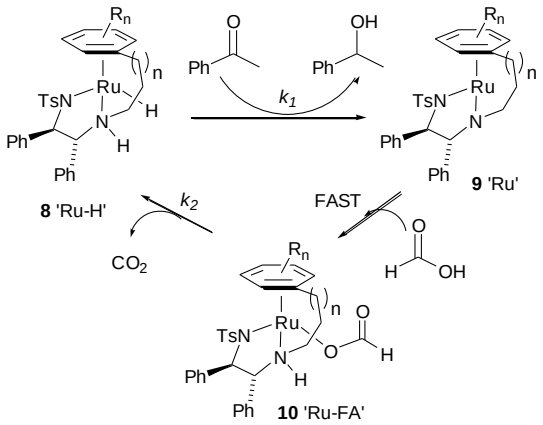

Scheme 2: Proposed three-step kinetic model for the ATH of ketones by Ru(II) catalysts.

The rate of reaction of **8** with ketone was assumed to be first order in both components, in accordance with the accepted mechanism of ketone reduction by ruthenium arene catalysts.[3] The rate of regeneration of **8** was assumed to be first order with respect to only the non-hydride catalyst. This is supported by the observation by Ikariya[7] that formic acid reacts quickly (a fast non-rate-determining reaction) with the 16 electron species **9** to give formate complex **10** which loses CO_2 in a unimolecular decomposition. The kinetic mechanism can therefore be abbreviated to a two-step kinetic model (Scheme 3) in which **'9'** represents both non-hydride ruthenium species (**9** and **10**).

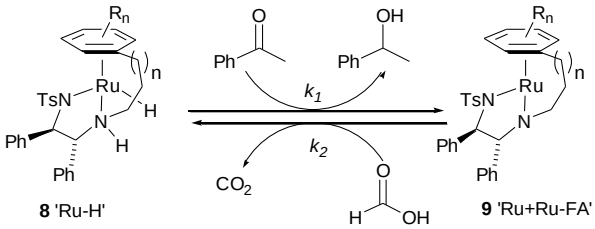

Scheme 3: Simplified two-step kinetic model for the ATH of ketones by Ru(II) catalysts.

The differential equations below describe the changes in [product] and [**8**] in accordance to the two-step kinetic model where the 'forward' reaction (i) is first order with respect to both [**8**] and acetophenone, and the 'backward' reaction (ii) is first order only with respect to [**9**].

$$\frac{d\,[\mathbf{8}]}{dt} = k_2\,[\mathbf{9}] - k_1\,[\mathrm{PhCOMe}][\mathbf{8}] \quad \text{(i)}$$

$$\frac{d\,[\mathrm{PhCOMe}]}{dt} = -\,k_1\,[\mathrm{PhCOMe}][\mathbf{8}] \quad \text{(ii)}$$

Under pseudo steady state conditions this combination of reaction orders has two major consequences:

a) At high concentrations of ketone, the rate of reaction of **8** is fast and the formation of **8** becomes the rate determining step. In this case, as the concentration of **9** is also constant, the reaction displays overall near-zero-order kinetics with respect to ketone.

b) At low concentrations of ketone (generally towards the end of the reaction), the ketone reduction reaction becomes rate determining. First order kinetics (with respect to ketone) would be expected to be observed at this stage.

The values of k_1 and k_2 thus determined for each catalyst in ATH of acetophenone to 1-phenylethanol, using curve-fitting software, are shown in Table 1.[5a] The most active catalyst was the "4C" tethered complex **3**, the high reactivity of which was a result of both a high rate of hydride (**8**) regeneration as well as a rapid rate of ketone reduction (i.e. high values of both k_1 and k_2). The other catalysts (**1**, **2** and **4-6)** showed a zero-order kinetic region at the start of the reduction and first-order kinetics with respect to ketone towards the end of the reaction. The untethered catalyst **7** also exhibited mixed-order kinetics similar to that of **3**.[5a]

Table 1: Summary of rate constants for acetophenone reduction using catalysts **1-7**.[a]

Entry	Catalyst	k_1 / M^{-1} min^{-1}	k_2 / min^{-1}
1	"2C" **1**	0.5	0.034
2	"3C" **2**	10	3.7
3	"4C" **3**	11	9.3
4	"5C" **4**	3.0	0.25
5	4-Me **5**	11	1.2
6	3,5-diMe **6**	2.5	1.6
7	Un-tethered **7**	0.75	1.0

a. Scheme 1 where Ar = Ph, R = Me, S/C 200, 40°C, 5:2 FA:TEA.

The X-ray crystallographic structure of (*R*,*R*)-**3** was obtained, as was that of the 4-Me substituted catalyst (*R*,*R*)-**5** (Figures 2 and 3 respectively). The X-ray structure of the 3C tethered complex (*S*,*S*)-**2** has already been reported[5b] (reproduced in Figure 4).

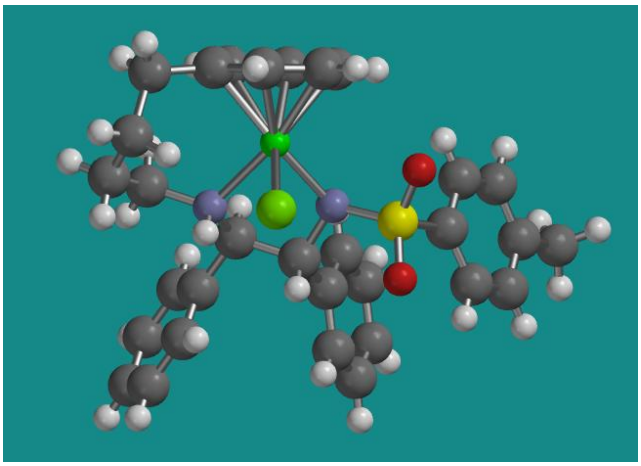

Figure 2 – X-ray crystallographic structure of (*R*,*R*)-**3**.

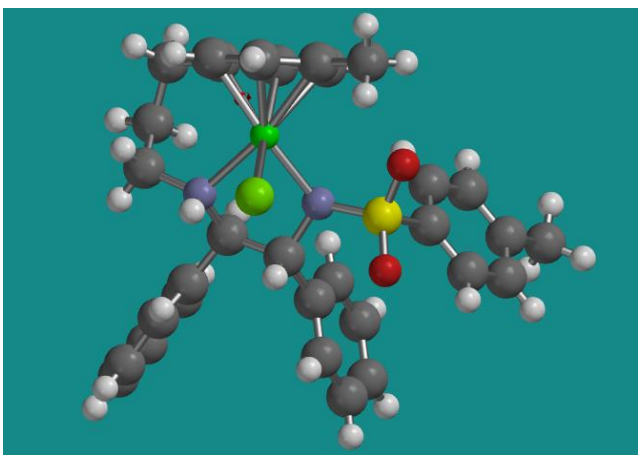

Figure 3 – X-ray crystallographic structure of (*R*,*R*)-**5**

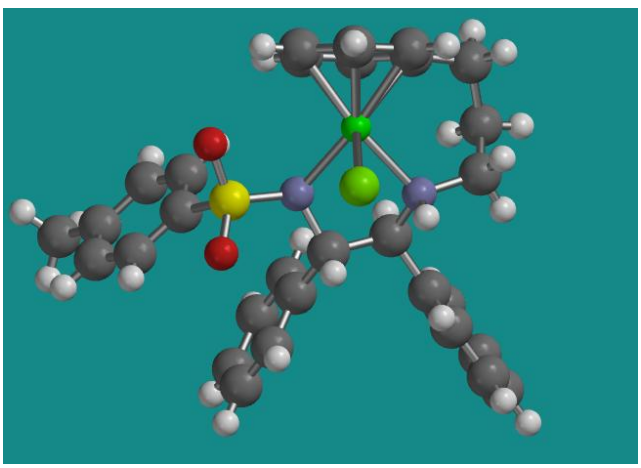

Figure 4 – X-ray crystallographic structure of (*S*,*S*)-**2**.[5b]

Comparison of the three structures (Figure 5, Table 2) reveals a close fit between the bond lengths and angles around the ruthenium atom for each complex. However it is apparent that

the longer side chain in **3** (with the highest values for k_1 and k_2) is oriented differently to that of the 3C tethered complexes **2** and **3** (which have similar values for k_1 and k_2). The view in Figure 5 compares the metal centred regions in each catalyst, in each case with the two nitrogen atoms (of the diamine ligand) eclipsing each other. Whilst **2** and **3** are essentially conformationally identical, with the tether away from the Cl atom, the '4C' tether in **3** is orientated towards the Cl atom, hence creating a larger steric obstacle in this region. Andersson *et al.* have demonstrated that the reactivity of a series of Ru(II) catalysts increases as the 'H-Ru-N-H' torsion angle decreases,[3d] which suggests that planarity of this group of atoms gives the best orbital overlap during the hydrogen transfer step. The steric requirements of the tethers may therefore enforce a subtle conformational change to this torsion angle, which in turn has a dramatic effect on catalyst reactivity. The values of the 'H-N-Ru-Cl' torsion angle (Table 2) reveal a trend that supports this, however the Ru hydride complexes may well have significantly different torsion angles. The sharp increase in k_2 (i.e. the rate of 'RuH' regeneration) measured for catalyst **3**, may also be a result of a conformation change facilitating the hydride formation.

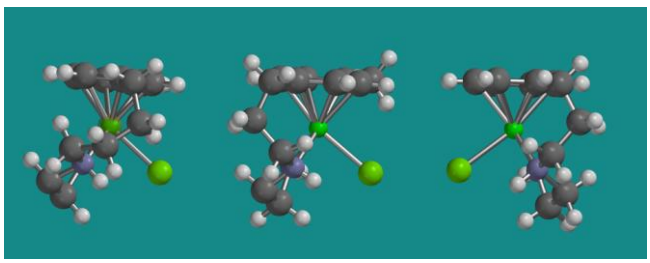

Figure 5. Comparison of the Ru-centred region of complexes (*R*,*R*)-**3**, (*R*,*R*)-**5** and (*S*,*S*)-**2** (tosyl and phenyl groups removed for clarity).

Table 2: Comparison of X-ray structural data for **2**, **3** and **5**.[a]

Dimension	**2**[b]	**3**	**5**[b]
Ru-N(H)	2.137(4)/ 2.134(4)	2.141(3)	2.149(4)/ 2.152(4)
Ru-N(Ts)	2.143(4)/ 2.144(3)	2.152(3)	2.144(4)/ 2.142(4)
Ru-Cl	2.4279(13)/ 2.4251(13)	2.4193(10)	2.4420(13)/ 2.4424(12)
NH-Ru-NTs	78.97(14)/ 79.29(14)	79.95(13)	78.69(14)/ 78.87(14)
Cl-Ru-NTs	88.40(11)/ 88.52(10)	88.01(9)	87.53(12)/ 86.23(11)
NH-Ru-Cl	81.79(11)/ 81.95(10)	80.96(10)	83.14(10)/ 82.84(10)
Cl-Ru-N-H	4.59/4.14	3.04 (3.13)	14.25 (3.78)/ 9.81 (4.11)

a. Complex **2** has been reported previously,[5b] complexes **3** and **5** are reported here for the first time, full data are in Supporting Information. b. The unit cell of **2** and **5** contains two slightly different structures, hence both dimensions are given.

Further kinetic studies were conducted using the most active tethered catalyst **3**. The dimeric precursor of **3** was used directly for this study without isolation of monomeric species, as it was demonstrated previously that with the incorporation of an 'aging' period, the results obtained for dimer and monomer are essentially identical.[5a] We have also previously demonstrated, through the repeated addition of fresh batches of substrate to the catalyst solution, that no significant catalyst decomposition takes place. Each batch of added substrate was fully reduced within a similar time frame, up to a total of 8 batches tested.[5f] In all cases, 0.01 mmol of dimer was used in 2 cm^3 of reaction solution (hence monomer catalyst concentration = 0.01 M). FA/TEA azeotrope was added to the initially measured ketone to give an overall volume of 2 cm^3. For each ketone concentration, the experiment was conducted twice to show the reproducibility of the reaction and to provide more accurate data. A summary of quantities added in each experiment is illustrated in Table 3.

Table 3: Summary of quantities of ketone and FA/Et_3N azeotrope added.

Entry	[Ketone] / M	Volume of Ketone / cm^3	Volume of FA/TEA / cm^3
1	0.1	0.024	1.976
2	0.5	0.116	1.884
3	1	0.234	1.766
4	2	0.466	1.534
5	3	0.700	1.300
6	4.5	1.050	0.950
7	6	1.400	0.600

Reactions with up to and including 3 M ketone concentration gave full conversions, however reactions at 4.5 and 6 M ketone concentrations did not. These two sets of data were therefore analysed separately.

Graph 1 shows the concentration of alcohol formed over time for initial ketone concentration 0.1 M to 3 M by catalyst **3**. In all cases, reactions were completed within 90 min. The rate constants, k_1 and k_2 were calculated for each experiment (Table 4) by the curve fitting method previously described.[5a] More accurate values of rate constants for catalyst **3** were also obtained from these data, and were determined to be: k_1 = 10, k_2 = 6 (RMS error = 0.070526).

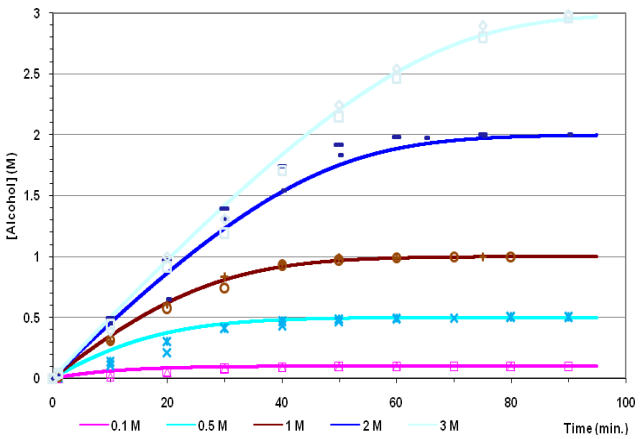

Graph 1: ATH of acetophenone at different concentrations up to 3 M by catalyst **3**. Complete conversions were achieved in these reactions.

Table 4: Rate constants calculated for experiments with initial ketone concentrations up to 3 M.

Entry	[Ketone] / M	k_1 / $M^{-1}min^{-1}$	k_2 / min^{-1}	Time /min.
1	0.1 [a]	5	2	50
2	0.5	6	5	55
3	1	8.5	6.5	60
4	2	8.5	7.5	70
5	3	7	6.5	90

a. Due to the low concentration of ketone, this entry may be subject to a larger error margin than the others. Calculated RMS error between experimental and theorietical curves for duplicate runs; 0.1M: 0.006662, 0.5M: 0.028897, 1.0M: 0.026818, 2.0M: 0.09078, 3.0M: 0.093721. Full data given in Supporting Information.

With the exception of entry 1, all the values calculated for k_2 are similar, and close to what would be predicted from a simple visual analysis of the early parts of the curves.[8] Entry 1 may be subject to a larger margin of error than the other values because it involved the use of a very dilute sample and solvent effects, e.g. viscosity, may have a greater effect.

For experiments with ketone concentration exceeding 3 M, the kinetic analysis must be treated in a different manner. In these cases, the amount of FA available is limited; the 2-step kinetic model can no longer be applied as the formation of formate complex **10** is no longer as fast and cannot be excluded from the rate equation. Because the 6M and 4.5M runs did not go to completion, the data was not fitted to theoretical models and no RMS error was calculated.

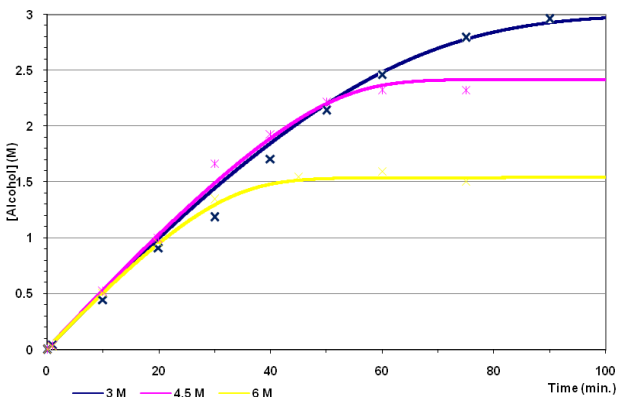

Graph 2: ATH of acetophenone at concentrations 3 M and above by catalyst **3**. Reactions exceeding 3 M did not reach complete conversion.

The concentration of FA used for reduction (i.e. the concentration of alcohol formed) was found to be limited by the amount of triethylamine present (i.e. $[Et_3N]_0$) which does not change significantly during the reaction. It was found that [FA] consumed in the reduction was 1.1 times that of the initial triethylamine concentration ($[Et_3N]_0$), and the reactions appear to come to a halt when this limit is reached (i.e. maximum [FA] used = ca. 1.1 x $[Et_3N]_0$). The final ratio of [FA]/$[Et_3N]$ at this point is hence ca. 1.4:1 (the initial ratio is 2.5:1). The concentrations of FA for each experiment are summarised in Table 5. The reasons for these observations are unclear, and are complicated by the release of gaseous H_2 from FA *via* the hydride complex (see below), but more studies are necessary in order to fully understand why this very specific excess of formic acid over the triethylamine is required for the reduction reaction to proceed. This will remain the subject of future studies in our groups.

Table 5: The concentrations of formic acid and their relationship with the amount of alcohol formed.[a]

Entry	[PhC OMe]	$[FA]_0$	$[Et_3N]_0$	[FA] used	Final [FA]	Final Ratio [FA]/[Et_3N]
1	6 M	3.45 M	1.4 M	1.54 M	1.9 M	1.36
2	4.5 M	5.46 M	2.2 M	2.42 M	3 M	1.36
3	3 M	7.5 M	3 M	3.3 M	4.2 M	1.4

a. $[FA]_0$ = inital concentration of formic acid, $[Et_3N]_0$ = inital concentration of triethylamine, [FA] used = concentration of formic acid used for reduction = concentration of alcohol formed. Final [FA] = $[FA]_0$ - [FA] used. Final Ratio [FA]/$[Et_3N]$ = Final [FA]/$[Et_3N]_0$

In order to gather more information about the factors influencing the kinetics of the reductions, the ATH of a series of 4-substituted acetophenones (**11-14**, and acetophenone; Scheme 4) were conducted using catalyst **3** in its dimeric form (followed by GC). In all cases, the reactions were conducted at 40 °C using 0.01 mmol of dimer at S/C = 200. Conversion vs time plots for these reactions are illustrated in Graph 3.

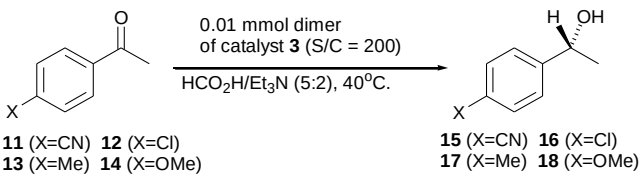

11 (X=CN) **12** (X=Cl)
13 (X=Me) **14** (X=OMe)

15 (X=CN) **16** (X=Cl)
17 (X=Me) **18** (X=OMe)

Scheme 4: The ATH of a series of 4-substituted acetophenones by catalyst (*R*,*R*)- **3**.

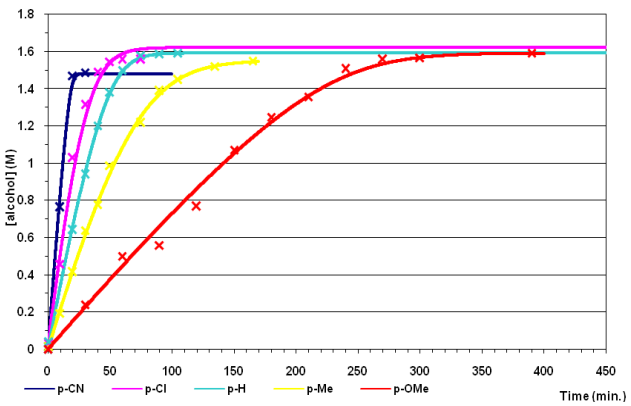

Graph 3: Conversion vs time plot for the ATH of a series of 4-substituted acetophenones by catalyst (*R*,*R*)-**3**.

All ketones were fully reduced in all cases and the ees did not change over the course of the reaction. With these data in hand, rate constants for each ketone reduction were calculated using the 2-step kinetic model (Table 6).

Table 6: Rate constants and e.e. obtained for ketone reductions in Scheme 4.[a]

Entry	Ketone	k_1 / $M^{-1}min^{-1}$	k_2 / min^{-1}	ee / %	Time / min.
1	X = CN (**11**)[b]	>30 [b]	12.0 [b]	83	20
2	X = Cl (**12**)	11.5	10.5	92	50
3	X = H	13.0	5.5	96	75
4	X = Me (**13**)	5.6	4.0	92	165
5	X = OMe (**14**)	4.2	1.1	96	330

a. See Graph 3. b. Due to the high rate of this reaction, there are too few data points to give an accurate curve-fitting result.

With an electron-poor substrate (Entry 1), high reactivity was observed, which decreases as the substituents become more electron-donating. However an unexpected outcome was observed; the value of rate constant k_2 was different for each ketone, which implies that the substrate may be directly involved in the **8** ('Ru-H') regeneration process. Note however that the value in entry 1 should be regarded with caution because the high rate provides very few points for accurate curve fitting. A possible explanation for this observation is the existence of a reverse reaction in which the reduced alcohol is re-oxidised back to the starting ketone, i.e. acting as a hydrogen source in competition with formic acid. Although there are precedents for Ru(II)-catalysed hydrogen transfers in related systems,[9] it would be unexpected as the formic acid should be the predominant reducing agent in this system. To investigate this, the reduction of acetophenone by catalyst **3** with 1-(4-methylphenyl)ethanol (**17**) (91 % ee (*R*)) added to the reaction, was followed by ^{1}H NMR spectroscopy. If acetophenone was reduced whilst 1-(4-methylphenyl)ethanol **17** was simultaneously oxidised then this would serve to confirm that product alcohol may be being re-oxidised back to ketone and therefore involved in the regeneration process of hydride **8**.

Following the reaction by ^{1}H NMR, with spectra recorded at the beginning, during, and at the end of the reduction reaction (see Supporting information for sample spectra) revealed that no formation of 4-methylacetophenone **13** was observed at any stage. However to confirm that it was not being missed due to overlapping peaks, an authentic sample of 4-methyl acetophenone (**13**) was added at the end (also shown in Supporting Information).

The pCH_3 peak in **13** appeared at a different position to the equivalent signal in **17** and would have been clearly visible if it had formed during the reduction. Hence there was no evidence for the oxidation of 1-(4-methylphenyl)ethanol (**17**) to 4-methyl acetophenone (**13**) during the course of acetophenone reduction to 1-phenylethanol. Having eliminated the possibility of substrate involvement, our attention turned to the significance of formic acid (FA) decomposition to the kinetics. Although such decomposition has long been known to take place in these reactions, i.e. through competing release of hydrogen gas from hydride **8** to regenerate **9**,[10,11] we had previously made the assumption that this was relatively negligible within the reaction time frame (typically less than 100 min at rt). For slower reactions, however, the decomposition of formic acid could significantly influence the reagent concentrations, i.e. as it is depleted. For less reactive ketones (X = OMe), and reactions with low initial concentrations of ketone (Table 4, entry 1), a higher proportion of the Ru-H **8** reacts with formic acid to give hydrogen to regenerate Ru-formate. However, since this is not taken into account in our model, the curve-fitting program would respond to this change by fitting a lower value of k_2 in these cases. It is therefore our speculation that, for slower reactions, the calculated value of k_2 is lower than the actual value due to the curve-fitting program. This is a limitation of the model that we shall address in future studies. The formic acid decomposition was selected for further investigation (see below).

Monitoring of ruthenium hydride by ^{1}H NMR during reduction of acetophenone catalysed by "4C" catalyst (3).

To gain further insights into the mechanism, we wished to study the formation of ruthenium hydride complexes during the reductions. In a typical experiment, the reduction of acetophenone was followed using ^{1}H NMR spectroscopy. The concentration of FA present was also followed prior to, and during, ketone reduction (Graph 4). Normally the ketone would be added at an earlier stage in the reaction. The concentration of FA decreases over time, as the formic acid is consumed in the conversion of the 16 electron species **9** to the ruthenium hydride **8** (blue), followed by dihydrogen release in the absence of substrate.[2b,10] This appears to be initially rapid, although the rate quickly levels off. When ketone is added, the concentration of formic acid drops more rapidly because **8** is being consumed in the reduction (red). The concentration of alcohol formed (pink) mirrors the decrease of formic acid. The high degree of FA reduction over an extended time would support our proposal for the effect on calculated k_2 values for slower reactions.

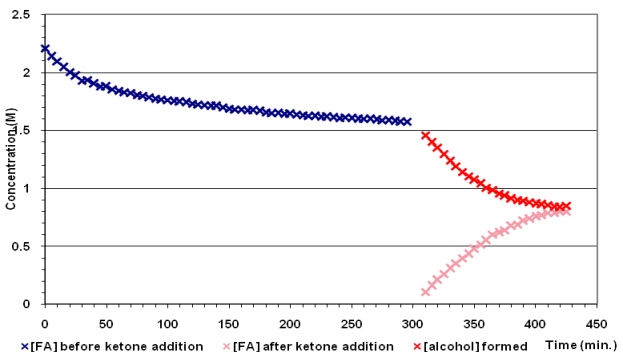

Graph 4: [FA] vs time plot before and after ketone addition. Ketone addition at Time = 300 min.

The use of a 700MHz spectrometer fitted with a cryoprobe provided a means to integrate the ruthenium hydride signals at ca. -5 ppm. The formation of Ru-H **8** was followed before ketone addition and was found to sharply increase up to ~0.0007M at which point it levelled off (Graph 5). When ketone was added, the concentration of **8** rapidly dropped as expected. During the reduction, the concentration of **8** builds

back up to its 'resting state' as ketone is consumed. These observations are in agreement with the 2-step kinetic model previously proposed (Scheme 3). Whilst this trend follows that which was predicted, the concentration of **8** was at all times below (ca. 30% of) that *calculated* for this experiment (0.00215M). Incomplete (30%) formation of Ru-H **8** is consistent with the continual depletion of the Ru-H **8** by reaction with formic acid to produce hydrogen. The remaining catalyst (70%) would therefore be Ru-formate forming a similar catalytic cycle to that proposed for the reduction of ketone. Further experimental studies in this area are underway. Alternatively the Ru-H **8**, due to saturation of the solution with hydrogen, may be capable of partially adding back to CO_2 (which will be present in high concentration in the solution) to reform formic acid (in a reversible process).[7]

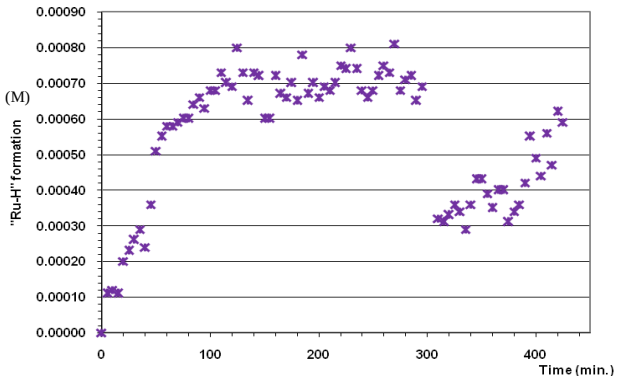

Graph 5: "**Ru-H**" formation vs time plot before and after ketone addition. Ketone addition at Time = 300 min.

In a previous publication,[5b] we demonstrated that the isolated hydride derivative of the '3C' tether complex **2** appears as two peaks, presumed to result from the formation of two diastereoisomers, in the region of -δ5.5 ppm, in a ratio of ca. 1:5. We wished to establish whether or not this ratio changed during the course of the reduction reaction.

In the current study, we employed the '4C' tethered complex **3**, since this gives improved results over **2** in terms of activity. A solution of **3** was prepared in formic acid/triethylamine (FA/TEA) 5:2 azeotrope and its conversion to the hydride form **8**, during the course of acetophenone reduction, was followed by 700 MHz ^{1}H NMR (an example spectrum is shown in the Supporting Information).

After ca. 30 minutes, there was evidence of hydride peaks corresponding to the two diastereoisomers seen for the 3C analogue **2**. Acetophenone (200 eq.) was added and the reaction was followed by NMR at regular intervals. A plot of the change in mol% 'RuH' (**8**) with time is illustrated (Figure 6), as is the conversion course of the reaction (Figure 7) and the ratio of the hydride isomers (Figure 8). The hydride concentration slowly increased during the reaction, levelling off at a concentration which reflected the resting level of 'RuH' following full consumption of the acetophenone. The catalyst is not deactivated; addition of further quantities of ketone reactivates the reduction reaction, in agreement with our previous studies.[5f] As in the previous example (Graph 5) the resting hydride concentration is below the theoretical maximum.

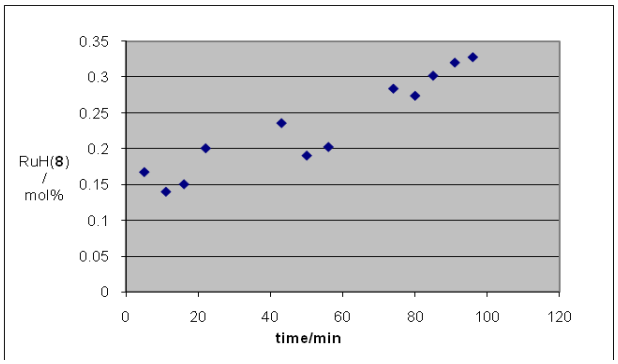

Figure 6: Level of RuH (**8**) expressed as mol% relative to initial ketone concentration during acetophenone reduction using catalyst **3** (S/C=200).

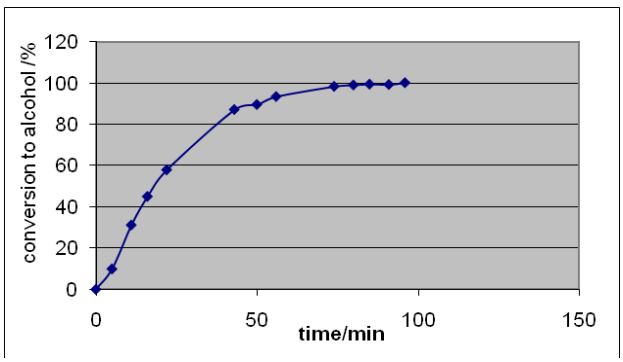

Figure 7: Time course of acetophenone reduction**.**

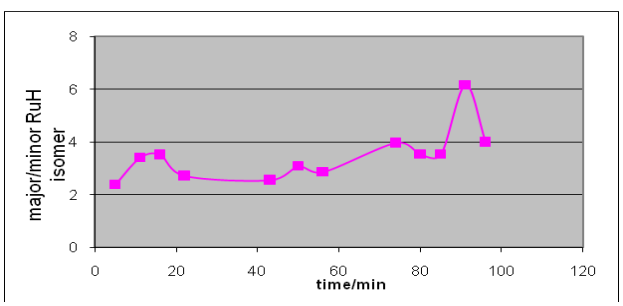

Figure 8: Change in ratio of 'Ru-H' peaks from **3** during reduction of acetophenone.

The ratio of the two hydride resonances (Figure 8) did not change appreciably during the course of the reduction reaction. This indicates that one diastereoisomer is significantly more reactive than the other, because the e.r. of the acetophenone reduction products is ca. 2:98. If each diastereoisomer was of similar reactivity, then the maximum ee (assuming opposite enantioselectivity) would be 50%.

Conclusions

In conclusion, we have found that Ru(II) complexes containing a tethering group between the diamine and the arene ligands, operate *via* a complex mechanism. Under typical reaction conditions (<3M ketone), the overall rate

depends upon the individual rates of the reduction and Ru-hydride formation steps. Small changes to the structure of the catalyst have a dramatic effect on the activity of the catalysts, presumably through conformational changes to the region around the catalyst active site. The simultaneous decomposition of formic acid has a significant effect upon the reaction kinetics for slower (>2h) reactions. Using a high field NMR instrument, it was possible to observe and measure, in real time, the relative quantity of 'Ru-H' species in solution during the course of a reduction reaction. Further studies are ongoing to establish the full details of the mechanism through which these catalysts operate.

Experimental.

General experimental details: All reactions, unless otherwise stated, were run under an atmosphere of argon at ambient temperature (18-22 ^{o}C). 0 ^{o}C refers to an ice slush bath and –78 ^{o}C refers to a dry ice-acetone bath. Heated experiments were conducted using thermostatically controlled oil baths. Reactions were monitored by TLC using aluminum backed silica gel 60 (F254) plates, visualized using UV 254 nm and phosphomolybdic acid, ninhydrin, potassium permanganate or vanillin dips as appropriate. Flash column chromatography was carried out routinely using 60 Å silica gel (Merck). Reagents were used as received from commercial sources unless otherwise stated. NMR spectra were recorded on a Bruker DPX (300 or 400 MHz) spectrometer. Chemical shifts are reported in δ units, parts per million (ppm) downfield from TMS. Coupling constants (*J*) are measured in Hertz. IR spectra were recorded on a Perkin-Elmer Spectrum One FT-IR Golden Gate. Mass spectra were recorded on a Bruker Esquire 2000 or a Bruker MicroTOF mass spectrometer. Melting points were recorded on a Stuart Scientific SMP 1 instrument and are uncorrected. Optical rotations were measured with an AA1000 polarimeter and are given in 10^{-1} deg cm^2 g^{-1}. Determination of enantiomeric excesses by GC analysis was achieved using a Hewlett Packard 5890A gas chromatograph, Hewlett Packard 3396A integrator and a Chrompac cyclodextrin-β-236M-19 50m or Chiracel β-DEX-120 25m column.

Procedure for the kinetic GC experiments, conducted at 40 °C: A solution of catalyst, either dimer (0.010 mmol) or monomer (0.020 mmol) was added to 5:2 HCO_2H:Et_3N azeotrope (2.0 cm^3). In the case of monomers this is stirred for ca. 45 min. at 40 ^{o}C, in the case of the dimers, overnight to permit the monomer to be fully formed. Acetophenone (480mg, 0.47 cm^3, 4.0 mmol) was added and the kinetics were followed taking samples at regular intervals which were immediately flushed through a pipette containing ca. 2 cm silica gel, using 1:1 EtOAc/hexane to elute. This process ensured the immediate removal of the catalyst from the reaction. The samples were analysed for conversion and e.e. using chiral G.C. The total volume of the solution was 2.47 cm^3, hence the catalyst total concentration is 0.0081 M, the S/C=200, and the initial ketone concentration/final alcohol concentration at 100 % conversion is 1.62 M.

Reduction procedure using tethered ruthenium diamine chiral ligands. A solution of ruthenium monomer (0.015 mmol) in formic acid/triethylamine (5:2) azeotrope (1.5 mL) was stirred in a flame dried Schlenk tube at 28˚C for 30 minutes. Ketone substrate (3.00 mmol) was added, and the reaction mixture was stirred at 28˚C for 3 hours. The reaction mixture was filtered on silica, washed (50% EtOAc/hexane) and concentrated under vacuum to give the reduction product. The residue was purified by flash chromatography where necessary. In kinetic experiments, samples were taken at the time points indicated and analysed by 1H-NMR spectroscopy or by chiral GC.

1-Phenylethanol: Enantiomeric excess and conversion by GC analysis (Chrompac cyclodextrin-β-236M-19 50m, T = 115 ^{o}C, P = 7 psi, ketone 13.2 min., *R* isomer 19.3 min., *S* isomer 20.3 min.); $[\alpha]_D^{22}$ +49.0 (c 1.0 in $CHCl_3$) 98% ee (*R*); δ_H(300 MHz; $CDCl_3$; Me_4Si) 1.47 (3 H, d, *J* 6.4, CH_3), 2.04 (1 H, br s, OH), 4.86 (1 H, q, *J* 6.4, PhC*H*CH_3), 7.33-7.35 (5 H, m, Ph); δ_C(75.5 MHz; $CDCl_3$; Me_4Si) 24.9 (q), 70.2 (d), 125.2 (2 x d), 127.2 (d), 128.3 (2 x d), 145.6 (s).

Procedure for the NMR reactions, conducted at 40°C: In a small Schlenk tube was added catalyst dimer (0.0125 mmol) or monomer (0.0250 mmol) in 5:2 HCO_2H:Et_3N azeotrope (2.5 cm^3). In the case of monomers this was stirred for ca. 30 min. at 40 ^{o}C, in the case of the dimers for a longer time to permit the monomer to be formed (normally overnight). 1 cm^3 of the above solution was transferred to a brand new NMR tube, and 0.05 cm^3 of d^6-benzene was added. Gently shaking of the NMR tube was required to mix in the benzene. (during shaking, an NMR cap *without* holes was fitted. After shaking, a NMR cap *with* holes was replaced). The tube was inserted into NMR spectrometer and locked on to the d^6 signal. Acetophenone (240 mg, 2 mmol, 0.235 cm^3) was added by syringe to the NMR tube. The time of addition was recorded. The NMR tube was shaked to mix in the substrate (cap *without* holes), and replaced with one *with* holes before placing it back in the NMR spectrometer to start the experiment. The NMR spectrometer was set to record at suitable intervals, e.g. 5-10 min. The total volume of the solution was 1.235 cm^3, hence the catalyst total concentration was 0.0081 M, the S/C=200, and the initial ketone concentration/final alcohol concentration at 100 % conversion was 1.62 M.

Data analysis: By using MestreC software, the conversion can be calculated by comparing the integration of the C**H**OH of the product (~4.7ppm) and the integration of the C**H$_3$** of the starting material (~2.45ppm).

Procedure for the attempted crossover reaction: To a solution of acetophenone (120 mg, 1 mmol) and 1-(4-methylphenyl)ethanol (136 mg, 1 mmol) in formic acid:triethylamine (5:2, 1 mL) and d6-benzene (0.05 mL) in an NMR tube (with a perforated top) was added catalyst **3** (6.2 mg, 0.01 mmol). The first NMR spectrum was recorded within 15 min and subsequent NMR spectra were recorded at 20 min intervals. The reduction of acetophenone could be clearly observed, whilst there was no evidence of concommitant oxidation of the alcohol. At the end of the reaction an authentic sample of 4-

methylacetophenone was added to identify the positions it occupied in the NMR spectrum. Sample spectra are given in the Supporting information.

Monitoring of formic acid decomposition and hydride formation during reduction: To a mixture of formic acid:triethylamine (5:2, 1 mL) and d6-benzene (0.05 mL) in an NMR tube (with a perforated cap) was added catalyst **3** (6.2 mg, 0.01 mmol). The first NMR spectrum was recorded within 10 min and subsequent 700 MHz NMR spectra were recorded at 5 min intervals. The decomposition of formic acid could be clearly observed and measured by integration of the formic acid:triethylamine ratio. After 300 minutes, acetophenone (240 mg, 2 mmol); reduction of acetophenone could be clearly observed and was followed by 1H-NMR.

Acknowledgements

We thank the EPSRC (Project Grant no. GR/S72214/1 to CL and Advanced Research Fellowship no. EP/D072182/1 to DJF) and AstraZeneca (collabrative studentship to FKC) for generous financial support of this project. Dr B. Stein and colleagues of the EPSRC National Mass Spectroscopic service (Swansea) are thanked for HRMS analysis of certain compounds. ALC was funding through the Erasmus European student exchange scheme. We acknowledge the use of the EPSRC Chemical Database Service at Daresbury.[12]

Notes and references

[a] *Asymmetric Catalysis Group, Department of Chemistry, University of Warwick, Coventry, CV4 7AL, UK. Fax: (44) 24 7652 4112; Tel: (44) 24 7652 3260; E-mail: m.wills@warwick.ac.uk.*

[b] *Cancer & Infection Chemistry, AstraZeneca, Mereside, Alderley Park, Macclesfield, Cheshire, SK10 4TG, UK.. E-mail: mark.a.graham@astrazeneca.com.*

† Electronic Supplementary Information (ESI) available: [Full kinetic data and graphs, and X-ray spectroscopic data]. See DOI: 10.1039/b000000x/

1. (a) M. J. Palmer and M. Wills, *Tetrahedron: Asymmetry* 1999, **10**, 2045. (b) R. Noyori and S. Hashiguchi, *Acc. Chem. Res.* 1997, **30,** 97. (c) S. E. Clapham, A. Hadzovic and R. H. Morris, *Coord. Chem. Rev*. 2004, **248**, 2201. (d) G. Zassinovich, G. Mestroni and S. Gladiali, *Chem. Rev.* 1992, **92**, 1051. (e) S. Gladiali and E. Alberico, *Chem. Soc. Rev.* 2006, **35**, 226. (f) T. Ikariya, K. Murata and R. Noyori, *Org. Biomol. Chem.* 2006, **4,** 393. (g) T. Ikariya and A. J. Blacker, *Acc. Chem. Res.* 2007, **40**, 1300

2. (a) S. Hashiguchi, A. Fujii, J. Takehara, T. Ikariya and R. Noyori, *J. Am. Chem. Soc*. 1995, **117**, 7562. (b) A. Fujii, S. Hashiguchi, N. Uematsu, T. Ikariya and R. Noyori, *J. Am. Chem. Soc.* 1996, **118**, 2521. (c) K. Matsumura, S. Hashiguchi, T. Ikariya and R. Noyori, R. *J. Am. Chem. Soc.* 1997, **119**, 8738. (d) K. Murata, K. Okano, M. Miyagi, H. Iwane, R. Noyori and T. Ikariya, *Org. Lett.* 1999, **1**, 1119. (e) K. J. Haack, S. Hashiguchi, A. Fujii, T. Ikariya and Noyori, *Angew. Chem. Int. Ed*. 1997, **36**, 285.

3. (a) M. Yamakawa, I. Yamada and R. Noyori, *Angew. Chem. Int. Ed.* 2001, **40**, 2818. (b) R. Noyori, M. Yamakawa and S. Hashiguchi, *J. Org. Chem.* 2001, **66**, 7931. (c) M. Yamakawa, H. Ito and R. Noyori, *J. Am. Chem. Soc.* 2000, **122**, 1466. (d) D. A. Alonso, P. Brandt, S. J. M. Nordin and P. G. Andersson, *J. Am. Chem. Soc.* 1999, **121**, 9580 (graph of rate vs dihedral angle). (e) P. Brandt, P. Roth and P. G. Andersson, *J. Org. Chem.* 2004, **69**, 4885. (f) J.-W. Handgraaf and E. J. Meijer, *J. Am. Chem. Soc.* 2007, **129**, 3099-3103.

4. (a) M. Wills, in 'Modern Reduction methods', ed. P. G. Andersson and I. J. Munslow, pp271, Wiley-VCH, Weinheim, 2008. (b) D. G. Blackmond, M. Ropic and M. Stefinvic, M. *Org. Proc. Res. Dev.* 2006, **10**, 457. (c) N. Uematsu, A. Fujii, S. Hashiguchi, T. Ikariya and R. Noyori, *J. Am. Chem. Soc.* 1996, **118**, 4916. (d) G. D. Williams, C. E. Wade and M. Wills, *Chem. Commun.* 2005, 4735. (a) J. B. Åberg, J. S. M. Samec and J.-E. Bäckvall, *Chem. Commun.* **2006**, 2771.

5. (a) F. K. Cheung, C. Lin, F. Minissi, A. L. Criville, M. A. Graham, D. J. Fox and Wills, M. *Org. Lett.* 2007, **9**, 4659. (b) A. M. Hayes, D. J. Morris, G. J. Clarkson and M. Wills, *J. Am. Chem. Soc*. 2005, **127**, 7318. (c) J. Hannedouche, G. J. Clarkson and M. Wills, *J. Am. Chem. Soc.*, 2004, **126**, 986. (d) J. E. D. Martins, G. J. Clarkson and M. Wills, *Org. Lett.* 2009, **11**, 847. (e) F. K. Cheung, A. M. Hayes, D. J. Morris and M. Wills, *Org. Biomol. Chem.* 2007, **5**, 1093. (f) D. J. Morris, A. M. Hayes and M. Wills, *J. Org. Chem.*, 2006, **71**, 7035.

6. (a) J. Wettergren, E. Buitrago, P. Ryberg and H. Adolfsson, *Chem. Eur. J.* 2009, **15**, 5709. (b) I. Plantan, M. Stephan, U. Urleb and B. Mohar, *Tetrahedron Lett.* 2009, **50**, 2676. (c) W. Baratta, G. Chelucci, S. Magnolia, K. Siega and P. Riga, *Chem. Eur. J.* 2009, **15**, 726. (d) J. Zhang, P. G. Biazecka, M. M. Bruendl and Y. Huang, *J. Org. Chem.* 2009, **74**, 1411. (e) Z. Ding, J. Yang, T. Wang, Z. Shen and Y. Zhang, *Chem. Commun.* 2009, 571. (f) M. B. Díaz-Valenzuela, S. D. Phillips, M. B. France, M. E. Gunn and M. L. Clarke, *Chem. Eur. J.* 2009, **15**, 1227. (g) X. Wu, J. Liu, D. D. Tommaso, J. A. Iggo, C. R. A. Catlow, J. Basca and J. Xiao, *Chem. Eur. J.* 2008, **15**, 7699. (h) A. Cortez, C. Z. Flores-López, R. Rodríquez-Apodaca, L. Z. Flores-López, M. Parra-Hake and R. Somananthan, *ARKIVOC*, 2005, 162. (i) A. V. Gaikwad, V. boffa, J. E. ten Elshof and G. Rothenberg, *Angew. Chem. Int. Ed.* 2008, **47**, 5407. (j) H. Takamura, J. Ando, T. Abe, T. Murata. I. Kadota and D. Uemura, *Tetrahedron Lett.* 2008, **49,** 4626. (k) C. Wang, X. Wu and J. Xiao, *Chem. Asian J.* 2008, **3**, 1750. (l) A. Pordea and T. R. Ward, *Chem. Commun.* 2008, 4239. (m) J. Wettergren, A. B. Zaitsev and H. Adolfsson, *Adv. Synth. Catal.* 2007, **349**, 2556.

7. (a) Koike, T.; Ikariya, T. *Adv. Synth. Catal*. 2004, **346**, 37. (b) Koike, T.; Ikariya, T. *J. Organomet. Chem.* 2007, **692**, 408.

8. We thank a referee for making the observation that for the runs at 2M PhCOMe and above, the initial rate (slope) is essentially constant, at ca. 0.05 M min^{-1}. This limiting rate should be equal to k_2[9] (assuming rate determining k_2) and so k_2 can be obtained by simply dividing the rate by catalyst concentration (0.01 M) to give k_2 = ca. 5 min^{-1}, which matches the curve-fitting calculation quite closely.

9. (a) C. P. Casey, T. B. Clark and I. A. Guzei, *J. Am. Chem. Soc.* 2007**,** **129**, 11821. (b) J. S. M. Samec, A. H. Éll, J. B. Åberg, T. Primalov, L. Eriksson and J.-E. Bäckvall, *J. Am. Chem. Soc.* 2006, **128**, 14293. (c) C. P. Casey and J. B. Johnson, *J. Am. Chem. Soc.* 2005, **127**, 1883. (d) C. P. Casey, S. E. Beetner and J. B. Johnson, *J. Am. Chem. Soc.* 2008, **130**, 2285 (e) J. Nyhlén, T. Primalov and J.-E. Bäckvall, *Chem. Eur. J.* 2009, **15**, 5220. (f) D. Mavrynsky, R. Sillanpää and R. Leino, *Organometallics*, 2009, **28**, 598. (g) A. Comas-Vives, G. Ujaque and A. Lledós, *Organometallics*, 2007, **26**, 4135. (h) B. Martín-Matute, J. B. Åberg, M. Edin and J.-E. Backvall, *Chem. Eur. J.* 2007, **13**, 6063. (i) A. Dijksman, J. M. Elzinga, Y.-X. Li, I. W. C. E. Arends and R. A. Sheldon, *Tetrahedron: Asymmetry*, 2002, **13**, 879.

10. (a) Y. Himeda, N. Onozawa-Komatsuzaki, H. Sugihara, H. Arakawa, and K. Kasuga, *J. Mol.Catal. A. Chemical* 2003, **195**, 95. (b) Soleimannejad, J.; Sisson, A.; White, C. *Inorg. Chim. Acta*. 2003, 121.

11. D. J. Morris and M. Wills, *Organometallics*, 2009, **28**, 4133–4140.

12. D. A. Fletcher, R. F. McMeeking and D. Parkin, *J. Chem. Inf. Comput. Sci*. 1996, **36**, 746.